Radio-frequency clock delivery via free-space frequency comb transmission

Ayshah Alatawi, Ravi P. Gollapalli, and Lingze Duan*

Department of Physics, University of Alabama in Huntsville, Huntsville, Alabama 35899, USA
**Corresponding author: lingze.duan@uah.edu*

Received August 11, 2009; revised September 29, 2009; accepted October 2, 2009;
posted October 6, 2009 (Doc. ID 115571); published October 27, 2009

We characterize the instability of an rf clock signal caused by free-space transmission of a frequency comb (FC) under typical laboratory conditions. The phase-noise spectra show the involvement of multiple random processes. For a 10 m transmission, the rms timing jitter integrated over $1-10^5$ Hz is 95 fs, and the root Allan variance over 1 s is 4×10^{-13}. The measured Allan variance has a τ^{-1} behavior and an excellent agreement with the phase noise measurement. These results indicate the feasibility of FC-based free-space rf clock distribution over short distances. © 2009 Optical Society of America

OCIS codes: 120.3930, 010.3310, 060.2605.

Precise time and frequency synchronization has become ubiquitously needed as the world enters the age of global connectivity. As the carrier frequencies of today's communication and computer networks continue to rise, the need for high-fidelity clock synchronization becomes imperative. Moreover, future networks will likely require enhanced flexibility in synchronization schemes to adapt to dynamic system topologies. Recently, there has been a growing interest in the study of the remote delivery of time and frequency references via fiber optic transmission of optical frequency combs (FCs) [1–4]. The rationale behind this concept is that, not only can frequency combs be directly anchored by the highly stable optical atomic clocks [5], they can also simultaneously transfer multiple (as large as $\sim10^5$) frequency references in both optical and microwave regimes [2]. With this motivation, it has been demonstrated that highly stable femtosecond lasers are able to deliver rf clock signals to distant locations with an instability of 7×10^{-15} at 1 s [1]. Meanwhile, femtosecond laser-based drift-free synchronization of optical and microwave sources has also been achieved through a fiber link [6].

Despite the current success, fiber optic FC clock transfer inherently relies on wired systems, which restrict its adaptability to dynamic networks. From this point of view, a wireless FC transfer scheme can be a useful alternative to the fiber optic scheme and offers some unique features, such as lower cost and better flexibility, which are particularly desirable for short-distance *ad hoc* clock distribution. As of today, however, there has been no report specifically addressing the feasibility of using free-space (atmospheric) FC transmission to deliver timing signals and the pertinent characteristics.

In the work reported here, we make the first attempt to characterize the rf clock instability caused by free-space FC transmission. We chose to set up our current experiment in the laboratory instead of an outdoor environment because of several considerations. First, a relatively quiet indoor environment likely leads to the lower limit of the transmission-induced instability, which serves the current research purpose of feasibility evaluation. Second, a major obstacle in laser atmospheric transmission is beam wandering due to air turbulence, which may inhibit precise phase-noise measurement [7]. A lab environment allows us to circumvent this problem so that a complete noise characterization can be made. Finally, there are potential applications that may involve the transmission of FCs in an enclosed space, which can be better simulated in a lab.

To measure the transmission-induced excess noise, we set up a double-pass free-space transmission link and a heterodyning detection system as shown in Fig. 1. The FC is provided by a commercial fiber laser (Precision Photonics FFL-1560), which generates 120 fs pulses at a repetition rate f_R of 90 MHz and an average power of 4 mW. The laser output has a 40 nm 3 dB bandwidth centered around 1560 nm, and its rf spectrum shows well-defined comb lines at the harmonics of f_R. The laser power is split at a fiber coupler, with 30% of the power going toward photodetector 1 and serving as the reference signal. The rest of the laser power is collimated to a 7 mm diameter beam and launched into the transmission link. The reflected beam is collected by a second collimator and coupled into photodetector 2. Both photodetectors have a 2 GHz rf bandwidth. We selected the tenth harmonic of f_R at 900 MHz as the center frequency for noise characterization. At such a high frequency, however, the bandpass filters we used are not

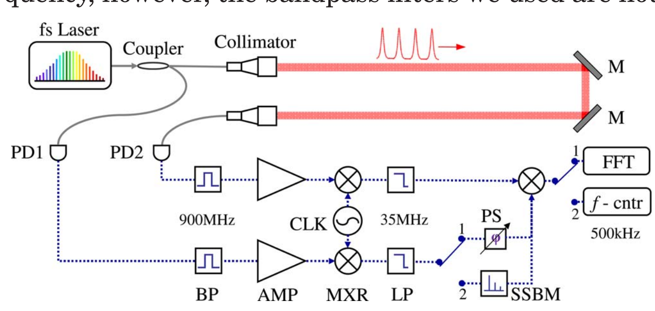

Fig. 1. (Color online) Schematic of the experimental setup. AMP, microwave amplifiers; BP, bandpass filters; CLK, clock; LP, low-pass filters; M, silver mirrors; MXR, mixers; PD, photodetectors; PS, phase shifter; SSBM, single-sideband modulator; FFT, fast Fourier transform analyzer.

0146-9592/09/213346-3/$15.00

able to sufficiently reject the adjacent harmonics, leaving multiple harmonics passing through both the signal and the reference arms. To improve the spectral selectivity, we use a clock generator (SRS CG635) as a local oscillator and mix the 900 MHz harmonic down to 35 MHz, where we can effectively filter out other frequency components with low-pass filters. Since the clock generator introduces only common-mode noise, it does not affect the differential measurement results. The resulted frequency signals serve two sets of characterizations. In phase-noise measurement, the 35 MHz signals from both arms are mixed in quadrature to generate a dc signal proportional to their phase difference. The fluctuation of this signal is then frequency analyzed with a fast Fourier transform analyzer (FFT, SRS SR785). In the second experiment, we frequency shift the reference signal by about 500 kHz with a single-sideband modulator (SSBM) before mixing it with the transmitted signal. The resulted 500 kHz beatnote is measured with a frequency counter (SRS SR620) to determine the Allan variance of the transmission-induced frequency variation. The SSBM is driven by a second clock generator, which, along with the first one, is phase-locked to an Rb-disciplined crystal oscillator (SRS FS725).

The transmission of a FC through the air can be treated as the propagation of an optical pulse train in a random continuum, where the refractive index is a continuous random function of position and time [8]. For the line-of-sight propagation of a laser beam in the air with weak fluctuation, it has been pointed out that a main source of excess phase noise is the temporal variation of the refractive index caused by transverse wind [8]. In our case, we believe that the fluctuation is largely caused by the air conditioning (AC) airflow, which predominantly moves downward from the ceiling and is perpendicular to the beam. In the experiment, we fix the total length of the transmission link ($\sim$10 m) but change the effective beam path exposed to the AC airflow by inserting rigid plastic tubes (2.5 cm inner diameter) into the beam path. We find that the tubes can effectively control the measured phase noise. We tested tubes with two open ends and tubes with optical windows attached to both ends (eliminating possible longitudinal wind inside the tubes), and discovered that the windows make little difference in the result. In addition, we also made measurements with the AC system off and found the noise to be much lower. These facts confirmed our hypothesis about the source of the excess noise. To evaluate the electronic system noise, we also measured the phase noise when the beam travels a negligible distance in the air.

The results of the phase noise measurement are summarized in Fig. 2. Figure 2(a) shows the transmission-induced timing jitter spectral density at four effective transmission distances as well as the system noise over a Fourier frequency range of 0.01 Hz to 100 kHz. A plot of the conventional single-sideband phase noise $\mathcal{L}(f)$ for 10 m transmission and the system noise is included in the inset. The system noise, attributed mainly to the rf amplifiers and the

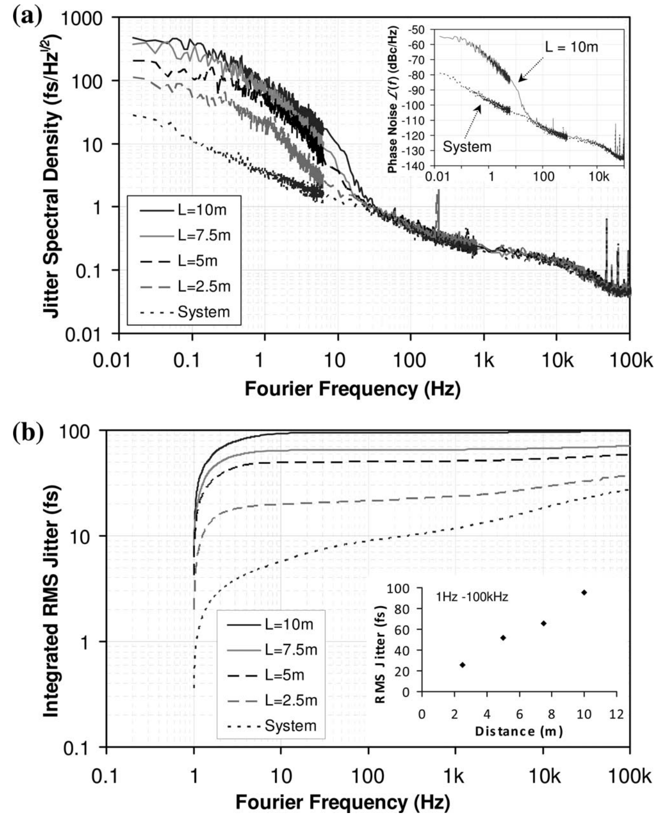

Fig. 2. Spectral density of the excess timing jitter for four effective transmission distances and the system noise; inset, single-sideband phase noise spectra for 10 m transmission and the system noise. (b) Integrated rms jitter for four transmission distances and the system noise; inset, the total rms jitter integrated from 1 Hz to 100 kHz versus effective transmission distance.

mixers, has a $1/f$ power frequency dependence below 1 kHz, indicating a flicker phase noise that commonly exists in rf amplifiers within this frequency range [9]. Between 1 and 100 kHz, the slope of the noise somewhat reduces, showing a gradual transition to white noise. The spike at 240 Hz is believed to be from the power line. The transmission-induced phase noise becomes appreciable above the system noise only when the Fourier frequency is below a few tens of hertz. As the frequency goes down, the power law of the noise gradually evolves from f^{-4} ($>$10 Hz) to f^{-2} (1–10 Hz) to f^{-1} (0.1–1 Hz) and eventually shows a trend toward f^{0} ($<$0.1 Hz). Such a behavior is markedly different from what has been observed in fiber optic systems [1]. It demonstrates the complexity of free-space FC transmission, which appears to involve multiple random processes [10]. To assess the rms jitter caused by the free-space propagation, we integrate the timing jitter spectrum from 1 Hz to 100 kHz. Figure 2(b) shows the integrated rms jitter versus the upper frequency limit of the integration for all five traces in Fig. 2(a). Over the full span ($1-10^{5}$ Hz), the total rms jitters are 37.5, 58.9, 71.2, and 99.0 fs for effective transmission distances of 2.5, 5, 7.5, and 10 m, respectively, and the total rms jitter caused by the system noise is 27.5 fs. The net transmission-induced jitters, with the system noise excluded, are of the same order as kilometerscale fiber optic transmission [1] and have an approximate linear relation over the propagation distance as shown in Fig. 2(b), inset.

The long-term transfer instability for 10 m transmission is characterized by measuring the root Allan variance σ_y of the beatnote frequency at a set of different averaging times, and the result is shown in Fig. 3. With the averaging time $\tau=1$ s, $\sigma_y=4.3\times10^{-13}$, which is 2 orders of magnitude smaller than a recent report on 100 m atmospheric rf clock transfer using direct modulation of a cw laser [7], but about 10 times greater than a similar comb-based transfer through 7 km of fiber [1]. As τ increases, σ_y descends at roughly τ^{-1}, which qualitatively agrees with the phase-noise measurement result at frequencies less than 1 Hz, i.e., flicker phase noise and white phase noise. To further confirm that the time-domain and the frequency-domain measurements agree with each other, we notice that Allan variance can actually be computed from the spectral density of phase noise according to the relation [10]

$$\sigma_y^2(\tau)=2\int_0^{f_h} S_y(f)\frac{\sin^4(\pi\tau f)}{(\pi\tau f)^2}\mathrm{d}f,$$

where f_h is the bandwidth of the system low-pass filter. Using the measured phase noise spectrum [Fig. 2(a) inset], we numerically calculate the Allan variance for 10 m transmission and find that it agrees very well with the measured result, as shown in Fig. 3. It should be noted that since we measure the phase noise only down to about 0.01 Hz and the two-sample variance filter function $\sin^4(\pi\tau f)/(\pi\tau f)^2$ peaks at $\tau f\sim0.4$, the calculated Allan variance is underestimated above $\tau=20$ s. This explains the discrepancy between the numerical and the measured results at the long averaging time. It is also interesting to realize that, although the transmission-induced frequency instability through air is much greater than in fiber, the Allan variance goes down much quicker in the air with increasing averaging time (τ^{-1} versus $\tau^{-1/2}$). For example, at 100 s, $\sigma_y\sim7\times10^{-15}$ for 10 m free-space transmission, which is already comparable with 7 km of unstabilized transmission in fiber [1].

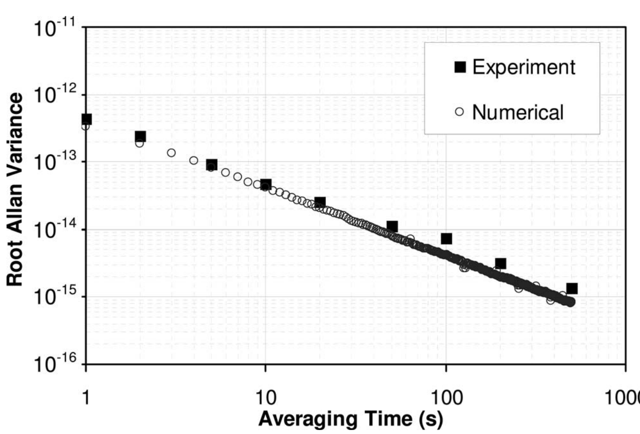

Fig. 3. Measured Allan variance with a 10 m effective transmission distance and the numerical estimation based on the phase-noise measurement.

Overall, the scale of the excess noise measured in the current experiment appears to have a reasonable agreement with other laser-based free-space rf clock transfer tests [7]. The exact physical processes that cause the shape of the phase noise and the τ^{-1} behavior of the root Allan variance are not completely clear at the moment, as most theories for optical pulse propagation in random media, to our best knowledge, have been developed to predict statistical quantities of single pulses [11]. From this point of view, the data presented here may offer a new angle to study the general problem of pulse propagation in random media. Although the experiment was performed in a specific setting of our lab, we believe the results still carry general significance because they set the scale of the excess noise for atmospheric rf clock transfer in a typical type of environment. We can conclude on the basis of our data that free-space FC-based rf clock transfer is feasible under normal indoor conditions for transmission distances at least of the order of tens of meters. With active noise control [1,2], this scale can be significantly longer.

The current experiment is somewhat hindered by the relatively large system noise, especially the flicker phase noise. Proper negative feedback has proved to be effective in lowering such noise [9]. Also, an effort is under way to assess this scheme in the open atmosphere, where it may find a broader range of applications.

References

1. K. W. Holman, D. D. Hudson, J. Ye, and D. J. Jones Opt. Lett. **30**, 1225 (2005).
2. S. M. Foreman, K. W. Holman, D. D. Hudson, D. J. Jones, and J. Ye, Rev. Sci. Instrum. **78**, 021101 (2007).
3. N. R. Newbury, P. A. Williams, and W. C. Swann, Opt. Lett. **32**, 3056 (2007).
4. G. Grosche, O. Terra, K. Predehl, R. Holzwarth, B. Lipphardt, F. Vogt, U. Sterr, and H. Schnatz, Opt. Lett. **34**, 2270 (2009).
5. Th. Udem, R. Holzwarth, and T. W. Hansch, Nature **416**, 233 (2002).
6. J. Kim, J. A. Cox, J. Chen, and F. X. Kaertner, Nat. Photonics **2**, 733 (2008).
7. B. Sprenger, J. Zhang, Z. H. Lu, and L. J. Wang, Opt. Lett. **34**, 965 (2009).
8. A. Ishimaru, *Wave Propagation and Scattering in Random Media* (Academic, 1978).
9. D. Halford, A. E. Wainwright, and J. A. Barnes, in *22nd Annual Symposium on Frequency Control* (1968), p. 340.
10. J. Rutman and F. Walls, Proc. IEEE **79**, 952 (1991).
11. L. C. Andrews and R. L. Phillips, *Laser Beam Propagation through Random Media*, 2nd ed. (SPIE, 2005).